Title
Silicon Carbide Platelet/Silicon Carbide Composites

Journal
Journal of the American Ceramic Society, 97(1)

Authors
Mitchell, T.
Jonghe, L.C. De
MoberlyChan, W.J.
et al.

Publication Date
1994-02-01

LBL-35185
UC-404
Preprint

Center for Advanced Materials

CAM

Submitted to Journal of the American Ceramic Society

Silicon Carbide Platelet/Silicon Carbide Composites

T. Mitchell, Jr., L.C. De Jonghe, W.J. MoberlyChan, and R.O. Ritchie

February 1994

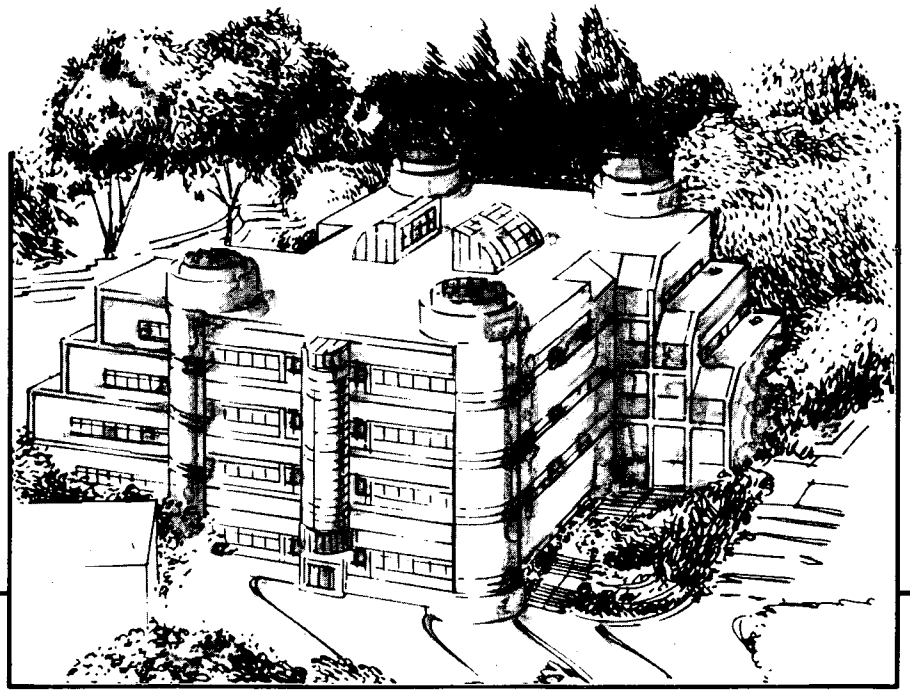

Materials and Chemical Sciences Division

Lawrence Berkeley Laboratory • University of California

ONE CYCLOTRON ROAD, BERKELEY, CA 94720 • (415) 486-4755

Prepared for the U.S. Department of Energy under Contract DE-AC03-76SF00098

DISCLAIMER

LBL-35185
UC-404

Silicon Carbide Platelet/Silicon Carbide Composites

Tyrone Mitchell, Jr., Lutgard C. De Jonghe,
Warren J. MoberlyChan, and Robert O. Ritchie

Materials Sciences Division
Lawrence Berkeley Laboratory
University of California
Berkeley, California 94720

February 1994

This work was supported by the Director, Office of Energy Research, Office of Basic Energy Sciences, Materials Sciences Division, of the U.S. Department of Energy under Contract No. DE-AC03-76SF00098.

SILICON CARBIDE PLATELET/SILICON CARBIDE COMPOSITES

Tyrone Mitchell, Jr., Lutgard C. De Jonghe, Warren J. MoberlyChan, and Robert O. Ritchie
Center for Advanced Materials,

Abstract

Alpha-silicon carbide platelet/beta-silicon carbide composites have been produced in which the individual platelets were coated with an aluminum oxide layer. Hot pressed composites showed a fracture toughness as high as 7.2 Mpa.$m^{1/2}$. The experiments indicated that the significant increase in fracture toughness is mainly the result of crack deflection and accompanying platelet pull-out. The coating on the platelets also served to prevent the platelets from acting as nucleation sites for the alpha to beta phase transformation, so that advantageous microstructure remains preserved during high temperature processing.

1. Introduction

The advantageous qualities of SiC in structural applications, such as its high elastic modulus, high thermal conductivity, and excellent oxidation resistance, are partly offset by its relatively low fracture toughness - typically around 3 MPa$\sqrt{m}$. A wide range of additives and particulate reinforcements have been tried as toughening agents, including TiB_2(1) or TiC(2) particles, and SiC or C fibers(3-5). The choice of toughening phases is restricted by high-temperature chemical incompatibility and by thermal expansion coefficient mismatch with the SiC. Reinforcement with SiC or C continuous fibers could possibly yield the highest high fracture resistance, but the use of such fibers is hindered by significant processing difficulties. Investigations of SiC particulate reinforcements in a number of ceramic matrix composites have shown that these can be effective in improving fracture toughness (6-10). While the results obtained with SiC whiskers in oxide matrix composites have been promising, potential health hazards in processing encourage directing attention to other forms of particulate reinforcement, in particular single-crystal platelets (11-14). The obvious compatibility of α-SiC platelets should make them the ideal reinforcing phase for a β-SiC matrix ceramic provided the matrix/platelet interface can be engineered to be less strongly bonded and the transformation of the β-SiC matrix from the α nuclei (15-17) can be inhibited. Under such circumstances a useful microstructural composite with enhanced fracture toughness might be obtainable.

The protection and isolation of the α-SiC platelets from the β-SiC matrix can be accomplished by the encapsulation of the reinforcing phase with alumina, prior to incorporation in the β-SiC powder. Alumina coatings on SiC powders have been obtained previously by Kubo et al (18). These authors achieved a uniform alumina additive distribution by an alkoxide powder coating

process, leading to a doubling of the MOR Weibull modulus, but found no effect on the fracture toughness which remained between 2.7-3.1 $MPam^{1/2}$. The method used here encapsulates α-SiC platelets prior to mixing with the β-SiC matrix powders, and involves controlled hetero-precipitation of an aluminum salt from an aqueous solution onto the platelet; calcination then converts the coating to alumina.

2. Experimental

2.1 Production of coated platelets

Coating of powder particles has been achieved by a variety of methods (18-25). A procedure, as described in the work of Kapolnek and De Jonghe (19) and by Mitchell and De Jonghe (20), was used in the present work.

A small amount of polymeric dispersant[1] was dissolved at room temperature in distilled water followed by the addition of SiC platelets.[2] After several minutes of ultrasonic agitation to disrupt agglomerates, the suspended platelets were added to a solution containing 0.1M aluminum sulfate hydrate and 0.2M urea in distilled water, in a flat bottomed boiling flask. This flask was then placed in a heating mantle, resting on a magnetic stirring plate. The suspension was vigorously stirred as the temperature was increased over a period of one hour to 83°C, and maintained in that condition for approximately 20 hours. The suspension was then cooled and allowed to settle. After the supernatant was discarded, the remaining solids were rinsed twice with acetone to remove most of the water. After drying, this powder was calcined in air at 1150°C for 4 hours to convert the coatings to α-alumina.

2.2 Compact Preparation

Submicron β-SiC powder[3] with an average grain size of 0.3 μm, was mixed in toluene with 6 wt% Al metal powder, 0.6 wt% B and 1 wt% C (added in the form of a wax which served both as the carbon source and binder). This powder mix was dried and sieved through a 325 mesh screen. Alumina-coated α-SiC platelets, average size 25 μm, were then dry-mixed with the β-SiC powder. The composite mix was then uniaxially compacted into 3.8 cm diameter discs under 35 MPa pressure to achieve a green density of approximately 55% of theoretical. The major impurities in the platelets are ~0.5%Al and 0.3% O.

---

[1]PVP K30, GAF Chemical Co., Wayne, NJ
[2]C-Axis Technologies, Quebec, Canada
[3]BSC -21, Ferro, Cleveland, OH

2.3 Hot Pressing

Dense composite discs were obtained by hot pressing at 1650°C and 50 MPa for 30 minutes using a graphite die, in a graphite element furnace, under flowing argon gas. The temperature was increased from room temperature to the final temperature at 10°C per minute. Pressure was applied at 1 MPa per minute up to 50 MPa, starting at 1000°C and released 5 minutes before the end of the isothermal hold period.

2.4 Mechanical Property Testing

A four point flexure test was used to measure bend strength. Five samples were cut from each hot-pressed or free-sintered specimen and were ground to 2.5 mm x 2.5 mm x 25 mm bars. These bend bars were surface polished to a 6 μm diamond finish and the tensile edges beveled to remove stress concentrations and any large edge flaws inflicted during sectioning. The outer and inner test spans were 19 mm and 6.4 mm, respectively. Bend strength was determined at a crosshead speed of 0.5 mm/sec.

The fracture toughness K_{Ic} was measured by creating an elliptical flaw on the tensile surface of the bend bars with a 150N Knoop indentation. The indentation was made such that the long axis of the indent was perpendicular to both the long axis of the bend bar and the applied stress axis. The fracture toughness value was determined from the relation (26):

$$K_{Ic}=(2\sqrt{\pi})\sigma(\sqrt{a}) \qquad (1)$$

where σ is the fracture stress and a the initial flaw radius obtained from the indentation.

2.5 Specimen Preparation for Microstructural Evaluation.

Hot pressed discs were diamond polished to 1 μm for optical or scanning electron microscopy. Some samples were etched with a boiling saturated solution containing equal parts NaOH and $K_3Fe(CN)_6$, prior to observation. Final densities were obtained using the Archimedes liquid-displacement method.

Samples were also sectioned parallel to the pressing direction and mechanically thinned for TEM analysis. To limit the effects of dissimilar ion etching rates of the various phases within the composite, samples were mechanically ground to electron transparency. Final argon ion milling of the TEM samples was used only to remove the mechancial polishing scratches.

3. Results and Discussion

3.1 Coating of SiC Platelets

Thick, uniform alumina precursor coatings were obtained on the SiC platelets by the controlled heterogeneous precipitation encapsulation process referred to earlier (19,20).

The coating first appeared as discrete grains on the surface of the SiC platelets and eventually grew to cover completely the surface with a layer approximately 500 nm thick, within a few hours (Figure 1). Once complete surface coverage has been obtained, the coating thickness is determined by the length of the process run. At the reactant concentrations used here, the coatings reached maximum thicknesses of 1 to 3 microns in 17 to 20 hours. The process run was limited to 20 hours to give the maximum coating thickness while lessening additional homogeneous precipitation in the bulk liquid.

Experiments run under standard conditions produced two different aluminum sulfate hydrate compounds. These compounds were $2Al_2O_3 \cdot SO_3 \cdot xH_2O$ (henceforth referred to as ASH-1) and $3Al_2O_3 \cdot 4SO_3 \cdot 9H_2O$ (henceforth referred to as ASH-2). These compounds were more easily identified when the nature of the precipitate was observed as a function of time. X-ray diffraction measurements of samples taken throughout a coating run showed a very large concentration of ASH-1 early in the process (up to about 4 hours), followed by increasing amounts of ASH-2. This very strongly suggests that ASH-1 precipitates first, followed by precipitation of ASH-2 due to a change in solution conditions. An explanation for the presence of the two compounds can be found by looking at the aluminum to sulfite ion ratios in each ASH molecule. The [Al(III)/SO_3^-] ratio is 4:1 in ASH-1 and drops to 1.5:1 for ASH-2. As nucleation begins, the aluminum cation concentration drops and as a result, products precipitated earlier have a higher proportion of aluminum in the ASH precipitate. This also offers an explanation for the tendency for ASH-2 to deposit when higher molar concentrations of aluminum sulfate hydrate are added to the starting solution (20).

The physical nature of the precipitate can be manipulated by changing the (stoichiometry) ratio of the urea concentration to the cation concentration in the starting solution. Moderate ratios (1:1 to 3:1) are practical for obtaining thick, crystalline coatings. The 1:1 ratio used here combined excellent process control with good yield, as close to 50% of the total concentration of aluminum ions in the original solution were precipitated.

The process can be accelerated through the use of higher stoichiometric ratios (above 3:1). However, the precipitate then formed is amorphous and covers the surface as a thin film instead of as discrete nuclei. This thin film grows to produce a coating of equivalent thickness in about half the time. However, crystalline coatings were preferred, as the amorphous coatings showed a tendency to crack severely on drying, which in turn could hinder their protective capabilities (Figure 2).

3.2 Hot Pressing

SiC-SiC platelet composites were hot pressed to full density with about 25 vol% coated platelets. The actual SiC platelet volume fraction, not including the alumina coating, was approximately 20 vol%. Higher loading with the 25 μm platelets resulted in poorer final density and nonuniform microstructures.

The hot pressed microstructure consists of the platelets and the fine β-grained matrix (grain size ≈1.0 μm) separated by the protective alumina phase (Figure 3). The spatial distribution of the platelets, achieved by careful dry mixing and milling, was not very uniform. Better distributions were obtained using wet processing methods to form the green body.

The alumina coating proved to be essential to the maintenance of platelet integrity. Figure 4 shows the microstructure of an etched SiC-SiC platelet composite hot pressed without the alumina coating on the platelets. The platelets, though not adversely affected by a phase transformation throughout the matrix, suffer from bonding fully to the matrix grains. As will be shown later, this prevents the platelets from contributing effectively to the toughening of the composite.

The alumina acts as a phase barrier in the composite, preventing the direct bonding between the matrix and the reinforcement. If direct bonding were to occur, the strength of the platelet-matrix interface would be equivalent to that of a SiC grain boundary. Though it is high in strength, the platelet will then not affect the fracture path significantly. Therefore, without the alumina coating, the resulting toughness of the composite must be expected to be similar to that of monolithic SiC.

The low processing temperature effected by the sintering additives largely suppressed the $\beta \rightarrow \alpha$ phase transformation, which occurs fast at 1950°C - the usual sintering temperature for SiC. The mechanism of the transformation has been examined in detail (15-17). The nucleus for this transformation would be the ubiquitous stacking disorder within the β grains. Once nucleated, the α grains grow very quickly due to the low energy interface between the $(111)_\beta$ plane and the $(0001)_\alpha$ plane. Rapid extension of this interface leads to large, plate-shaped α grains. Without the presence of an alumina coating, the α-SiC platelets in the composite would serve as efficient nucleation sites for the phase transformation, providing a mechanism for their destruction by the transforming β-SiC. Despite the low processing temperature this could have been a problem. The sintering aids that allow low temperature hot pressing of the SiC, chiefly aluminum, also lower the temperature of the phase transformation. However, no evidence of an aluminum-catalyzed transformation was seen.

3.3 Transmission Electron Microscopy.

Transmission electron microscopy (TEM) confirmed optical and SEM microscopy results by showing nonuniform spatial distribution of platelets (i.e. platelets were often grouped together). Occasional grouped platelets lay face-to-face, without alumina between them, thereby suggesting some platelets agglomerated during the coating process. Many platelets were aligned within the TEM cross sections with the platelet faces perpendicular to the hot pressing axis. Figure 5 shows a section of an α-SiC platelet with an alumina coating, surrounded by fine grains of the β-SiC matrix. The alumina grains provided a continuous coating, typically one to two grains thick, along the platelet faces. High resolution electron microscopy (HREM) imaging detected no alteration of the original 4-H structure of the alpha platelets. The lattice image in Figure 5b depicts the typical 4-H stacking, with occasional stacking defects as noted by arrows. The interface was not atomically flat along the entire face of the platelet, probably reflecting features of the irregular faces of the initial platelets. No intermediate phases between alumina and (0001) surfaces of the SiC platelets were detected by electron diffraction nor by HREM. In particular, mullite, which would be the expected phase resulting from reactions between possible silica at the surface of silicon carbide powders and alumina, could not be detected on either side of the alumina layer.

It was noted that alumina grains neighboring the α-SiC plates often exhibited low angle boundaries. Also, major bend contours often crossed from SiC platelet into alumina grains, indicating that some orientation relationships might be present. The details of these relationships were expected not to be of immediate relevance in the properties of the composite, and presently were not further explored.

The solid solubility of Al in SiC at the sintering temperature of 1650°C is approximately 1 wt% (29). The 5 wt% Al (plus B and C-black) added to aid sintering has been suggested to form an $Al_8B_4C_7$ compound which then segregates in small cavities within the matrix. Previous investigations (30) have indicated the presence of this compound based on limited XRD data and optical metallography. The TEM micrograph in Figure 6 depicts a large, irregular grain, which was determined to contain Al, B and C based on EELS spectroscopy. The interpenetrating morphology of this grain suggested it was present as a liquid phase during hot pressing. Electron diffraction of this phase and lattice imaging (Figure 6b) were consistent with the presence of the hexagonal superlattice of the $Al_8B_4C_7$ structure. These Al-B-C rich grains, as well as other B-C rich grains not shown, did not constitute a large volume fraction of the matrix. Coupled with the limited solubility of Al in SiC, the TEM analyses indicated that a significant fraction of the added aluminum metal may have escaped during hot pressing or has simply added to the alumina phase along the platelets.

Figure 7 depicts a typical grain boundary between SiC grains, with lattice fringes from both grains extending into the interface. Since the grain boundary was not parallel to the electron beam, the presence of thin amorphous phases < 1 nm, while unlikely, could not be ruled out with

certainty. The Moiré fringes resulting from overlapping crystals indicate the grain boundaries are not planar even over distances of tens of nanometers, and also suggest only crystalline material is present. No amosphous phase was observed between β-SiC grains of the matrix, nor between grain boundaries of phases formed by the sintering additives such as $Al_8B_4C_7$, (Figure 6b). (A more detailed description of the interfaces between platelets and the alumina coating is underway.)

Also depicted in Figure 6 is a portion of an atypically large SiC grain. Most SiC grains within the matrix were 0.1 to 0.5 microns in diameter. However, occasional bulk grains were larger than 2 microns in length. The presence of such grains suggested that some "abnormal" grain growth had occurred during sintering. Electron diffraction (and XRD) established that these grains remain as β-SiC; however, they often appeared twinned with a lower density of stacking defects than was present in the fine β-SiC grains.

3.4 Mechanical Property Testing

The measured toughness and strength values of the alumina-coated SiC platelet - SiC composites were significantly higher than in monolithic SiC; specifically, the composite samples displayed a maximum fracture toughness, K_c, of up to 7.3 MPa$\sqrt{m}$ with bend strengths, σ_b, up to a maximum of 738 MPa. Average property values of $K_c \approx 6$ MPa$\sqrt{m}$ and $\sigma_b \approx 650$ MPa compare favorably with values reported in the literature for 20-25 vol% loaded SiC-TiC particulate composites (1,2). The present results on alumina-coated SiC_p-SiC composites are compared with those for monolithic SiC and the best data from other studies in Table I. It is apparent that without the alumina coating, the properties of SiC-platelet reinforced SiC are essentially the same as unreinforced SiC.

Such toughness results can be rationalized in terms of the effects of the relative strength and toughness of the matrix, reinforcement and interface, following the approach of Becher (27). This treatment separates the toughening contributions in composites containing brittle, elastic, discontinuous reinforcements into two components, namely toughening due to the matrix and crack-tip shielding (resistance-curve toughening) due to the reinforcement. The toughness of the composite, defined either in terms of a stress intensity, K_c^c, or J-integral, J_c^c, is therefore expressed as:

$$K_c^c = (E^c J_c^c)^{1/2} = [E^c(J_c^m + \Delta J^s)]^{1/2}, \qquad (2)$$

where E^m and E^c are, respectively, the Young's modulus of the matrix and of the composite K_c^m and J_c^m define the matrix toughness:

$$J_c^m = (K_c^m)^2 / E^m, \qquad (3)$$

and ΔJ^s is the energy associated with crack-tip shielding, in this case from crack bridging and pullout:

$$\Delta J^s = \Delta J^b + \Delta J^{po} \tag{4}$$

In Eq. 4, ΔJ^b is the toughening contribution from the actual bridging of the crack by the reinforcement phase, and ΔJ^{po} is the toughening induced if this phase pulls out in the crack wake, instead of fracturing. Note that this expression assumes that the toughness of the composite results solely from the sum of the matrix toughness and the crack-tip shielding. It does not take into account toughening contributions due to the reinforcement phase from crack deflection and branching, and crack trapping by, or crack renucleation across, the phase; these "non-shielding" mechanisms do not induce R-curve toughening, but instead act to increase the J^m term without affecting ΔJ^b.

For large-aspect ratio (i.e., short fiber) reinforcements where the thermal expansion coefficient of the matrix exceeds that of the fiber, the resulting compressive stress on the fiber leads to frictional forces along the debonded fiber/matrix interface, such that DJ^b becomes (27).

$$\Delta J^b = [(\sigma_F^l)^3 r f_v] / 6 E^l \tau_i, \tag{5}$$

where σ_F^l and E^l are, respectively, the strength and modulus of the fiber ligaments; r is the ligament radius; f_v is the volume fraction of bridging ligaments (equal to the fiber volume fraction if all reinforcements are aligned perpendicular to the crack); and τ_i is the frictional shear resistance of the interface, given by the product of the coefficient of friction, μ, and the stress, σ_R, imposed on the interface due to radial mismatch in thermal expansion mismatch ($\tau_i = \mu\sigma_R$).

Similarly, the energy contribution associated with the pullout of a fiber-like reinforcement can be expressed in terms of the area fraction of pullouts, A^{po}, and the pullout length, $l^{po} \approx r\sigma_F^l/2\tau_i$, as:

$$\Delta J^{po} = A^{po} \tau_i . r (l^{po}/r)^2 \tag{6}$$

Adapting Eqs. 5 and 6 for platelet reinforcements, of diameter d and width w (where $d/w \sim 5$), i.e., by setting $r = wd/(w + d)$, yields:

$$\Delta J^b = [(\sigma_F^l)^3 w d f_v] / (w + d) 6 E^l \tau_i, \tag{7}$$

and

$$\Delta J^{po} = A^{po} \tau_i . (l^{po})^2 (w + d)/wd. \tag{8}$$

However, for the present case of SiC platelets where there is no significant thermal expansion mismatch between the matrix and reinforcement, the absence of interfacial friction between the

partially debonded reinforcement and the matrix means that the bridging component results primarily from elastic stretching of the bridging ligaments, i.e,

$$\Delta J^b = [(\sigma_F^l)^2 \, f_v \, l^{db}] / 2 \, E^l . \qquad (9)$$

In this expression, l^{db} is the debonded length along the matrix/ligament interface, which can be defined as (27):

$$l^{db} = r \gamma^l / 6 \gamma^i \approx w \, d \gamma^l / 6 \, (w + d) \gamma^i , \qquad (10)$$

where γ^l/γ^i is the ratio of the fracture energy of the bridging ligament to that of the matrix/ligament interface.

Thus, taking $\Delta J^{po} \approx 0$ because the thermal expansion mismatch stress between the matrix and reinforcement will be small, the toughness of the SiC-SiC composite can be expressed as:

$$K_c^c = [E^c \{ J_c^m + (\sigma_F^l)^2 \, f_v \, w \, d \gamma^l / 12 \, (w + d) \, E^l \gamma^i \}]^{1/2} . \qquad (11)$$

To evaluate Eq. 11 for the present composites, we take the composite modulus to be 450 GPa and consider 20 vol% of bridging platelets of thickness ~4 μm and width ~25 μm, with a strength of 8 GPa and a modulus of 500 GPa. The debonding length can be approximated by estimating the fracture strength of the platelet to be roughly 15 times that of the matrix-reinforcement interface (as in monolithic SiC), such that the toughness due to elastic bridging becomes $\Delta J^b \approx$ 110 J/m^2. Thus, since the matrix toughness is $K_c^m \approx 3$ MPa$\sqrt{m}$ (equivalent to $J_c^m \approx 22$ J/m^2), a composite toughness of approximately $K_c^c \approx 7.7$ MPa$\sqrt{m}$ is predicted. Experimentally measured fracture toughness values (Table I) clearly approach these predicted values. Specifically, observations of crack profiles (Figure 8) show an extremely jagged, branched crack path which circumvents the platelets. In addition, fracture surfaces (Figure 9) reveal pullout lengths of the order of 10 to 15 μm, comparable to the predicted value of $l^{po} \sim 9$ μm used in the above calculations.

The above treatment for the SiC_p-SiC composites has not considered the role of the alumina coating. Since there are differences in thermal expansion coefficients between the alumina, SiC platelets and the matrix, cooling during processing will result in a larger contraction of the alumina coating than of either the platelet or matrix. This should result in a residual compressive stress on the platelet, a tensile hoop stress on the alumina coating, and a stress on the matrix that is tangentially compressive and radially tensile all of which might be expected to induce a frictional component to bridging from the contraction of the alumina coating onto the SiC platelets. However, because of the state of residual tension in the coating, the platelet may be somewhat strengthened and the alumina effectively weakened. As a result, the weakened matrix-reinforcement interface, which increases the γ^l/γ^i term, alternatively promotes crack deflection around the perimeter of the platelets. This is evident in the increased crack branching around

platelets and larger pullout lengths in the alumina-coated SiC_p-SiC composites, in contrast to composites containing uncoated platelets where crack paths resemble those in monolithic SiC with little evidence of crack deflection.

It should be noted, however, that the mechanical properties of the composite will be sensitive to processing variables. For example, hot pressing produces definite platelet orientation, with the faces of many platelets aligned somewhat perpendicular to the pressing direction. The properties described in this study were obtained with the loading direction aligned parallel to the pressing direction, such that crack propagation is perpendicular to the platelet faces. This clearly promotes optimal toughness properties; in contrast, for orientations where crack propagation is parallel to the platelet faces, measured toughness values were not much higher than in monolithic SiC. There can be an additional effect associated with the surface roughness of the platelets. To develop the best toughness properties, platelet surfaces should be smooth to enhance interfacial sliding; when platelets with jagged rough surfaces were used (Figure 10), toughnesses were lower. Also, care must be taken in processing to limit the occurrence of silica, which can form on SiC due to the calcination of the alumina-coated platelets or in the SiC matrix from grinding of the SiC powder. The presence of silica can degrade the properties of the matrix; moreover, silica layers have been clearly shown to reduce the benefits of SiC whiskers in previous studies on ceramic-matrix composites (28).

4 Conclusions

In addition to easing the barriers to densification as for alumina-SiC composites, coating SiC platelets with alumina has been shown to provide protection to the SiC platelet in SiC-SiC composites. This allows the platelet to survive densification without directly bonding to the SiC matrix. This resulted in higher strength and toughness values. In addition to protection, the alumina coating also plays a beneficial role in crack bridging and interface debonding.

The β-SiC-SiC platelet composites showed high bend strengths and high fracture toughness. The presence of the alumina coating appeared to lead to deflection of the crack path, as opposed to the behavior of non-coated SiC platelet composites which showed no crack deflection. The SiC-SiC composites, however, were sensitive to surface morphology of the platelets and possibly to processing variables such as the amount of silica present in the matrix or on the platelet surface. To achieve consistently good properties, these factors as well as the quality of the platelet distribution must be observed.

References

1. Y. Murata, and G. Weber, "Sintered Silicon Carbide -titanium diboride mixtures and articles thereof," US Patent 3,340,020 (1982).
2. G. C. Wei, P. F.Becher, "Improvement in Mechanical Properties in SiC by the Addition of TiC Particles," *J. Am. Ceram. Soc.*,**67**(8), 571-574 (1984).

3. P. Lamicq, G. Berhart, M. Daucher, J. Mace, "SiC-SiC Composites," *Am. Ceram. Soc. Bull.* **65**(2), 336-338 (1986).
4. E. Fitzer, R. Gadow, "Fiber-reinforced Silicon Carbide," *Am. Ceram. Soc. Bull.* **65**(2), 326-335 (1986).
5. L. Héraud, P. Spriet, "High Toughness C-SiC and SiC-SiC Composites in Heat Engines," *Whisker and Fiber -Toughened Ceramics*, Eds.: R. Bradley, D. Clark, D. Larsen, and J. Stiegler, ASM Internat. , 1988, pg 217-224.
6. G. C. Wei, and P. F.Becher, "Development of SiC-Whisker-Reinforced Ceramics," *Am. Ceram. Soc. Bull., 64( )*, 298-304 (1985).
7. J.R.Porter,.; F.F.Lange. ; A.HChokshi. ., "Processing and Creep Performance of SiC-Whisker-Reinforced Al_2O_3," *Am. Ceram. Soc. Bull.*, **66**( ), 343-347 (1987).
8. Homeny, J.; Vaughn, W.L.; Ferber, M.K., "Processing and Mechanical Properties of SiC-Whisker-Al_2O_3-Matrix Composites," *Am. Ceram. So. Bull.* **66**( ), 333-338 (1987).
9. J. Homeny, and W.L. Vaughn, " Whisker Reinforced Ceramic Matrix Composites," *MRS Bull.*,**7**(7), 66-71(1987).
10. Tiegs, T. N.; Becher, P. F., "Sintered Al_2O_3,-SiC-Whisker Composites," *Am. Ceram. Soc. Bull.* **66**( ), 339-342 (1987).
11. Chou, Y.S.; Green, D.J., "SiC-Platelet/Al_2O_3, Composites," *J. Amer. Ceram. Soc.* 75(12), 3346-3352(1992).
12. N. Claussen, "Ceramic Platelet Composites", *Proceedings of the 11th RISO International Symposium on Metallurgy and Materials Science 1990, Structural Ceramics Processing Microstructure and Properties*, 1990.
13. C. Nischik, M. M. Seibold, N. A.Travitzky, N.Claussen, "Effect of Processing on Mechanical Properties of Platelet-Reinforced Mullite Composites," *J. Am. Ceram. Soc.* **74**(11), 2464-2468(1991).
14. D. Baril, S. P. Tremblay, and M. Fiset," Silicon Carbide platelet-reinfiorced silicon Nitride composites," *J. Mater. Sci.* **28**, 5486-5494 (1993).
15. A. H. Heuer, G. A. Fryburg, L. U. Ogbuji, T. E.Mitchell, S. Shinozaki,,"$\beta \rightarrow \alpha$ Transformation in Polycrystalline SiC: I, Microstructural Aspects" *J. Am. Ceram. Soc.* **61**(9-10), 406-412 (1978).
16. T. E. Mitchell, L.U.Ogbuji, A. H Heuer, "$\beta \rightarrow \alpha$ Transformation in Polycrystalline SiC: II, " *J. Amer. Ceram. Soc.*, **61**(9-10), 412-413 (1978).
17. T. E. Mitchell, L.U. Ogbuji, A.H. Heuer, , "The $\beta \rightarrow \alpha$ Transformation in Polycrystalline SiC: III, The Thickening of α Plates," *J. Am. Ceram. Soc.* **64**(2), 91-99 (1981).
18. H. Kubo, H. Endo, K. Sugita, "Sintering Behavior of Ultra-Fine Alumina-Coated Silicon Carbide," *Proc. 1986 Internat. Conf.- P/M '86-, Düsseldorf, July7-11*, pp1151-1154, (1986).
19. D. Kapolnek, L.C.De Jonghe, "Particulate Composites from Coated Powders ," *J. European Ceram. Soc.* **7**, 345-351, (1991).
20. T. D.Mitchell, Jr., L. C. De Jonghe, " Alumina-SiC composites from Coated Powders", *J. Am. Ceram. Soc.,* in press (1994).

21 C-L. Hu and M.N.Rahaman, "SiC-Reinforced-Al_2O_3 Composites by Free Sintering of Coated Powders," *J. Amer. Ceram. Soc.*, **76**(10),2549-2554(1993).
22. M. D. Sacks, N. Bozkurt, and C.W. Scheiffele, "Fabrication of Mullite and Mullite Matrix Composites by Transient Viscous Sintering of Composite Powders," *J. Amer. Ceram.* Soc., **74**(10), 2428-2437(1991)
23. E. Matijevic, "Preparation and Interactions of Colloidal Particles of Interest in Ceramics," in *"Ultrastructure Processing of Advanced Ceramics,"* J.D. Mackenzie and D.R. Ulrich, Eds, J.Wiley, New York (1988), pp 429-442.
24. A.K.Garg and L.C. De Jonghe, "Microencapsulation of Silicon Nitride Particles with Yttria and Yttria-Alumina Precursors," *J. Mater.Res.*, **5**(1), 136-142 (1990).
25. H. Okamura, E. A. Barringer, and H. K. Bowen,"Preparation and Sintering of Monosized Al_2O_3-TiO_2 Composite Powders," *J. Amer. Ceram. Soc.*, **69**(1), C22-24 (196).
26. P C. Paris, G.C. Sih, *ASTM STP* **381** 1965, 30-81.
27. P.F.Becher, " Microstructural Design of Toughened Ceramics ," *J. Am. Ceram. Soc.*, **74**(2), 255-69 (1991).
28. Homeny, J.; Vaughn, W.L.; Ferber, M.K., "Silicon Carbide Whisker/ Alumina Matrix Composites: Effect of Whisker Surface Treatment on Fracture Toughness," *J. Am. Ceram. Soc.*, **73**(2), 394-402 (1990).
29. Tajima, Y.; Kingery, W.D., "Solid Solubility of Aluminum and Boron in Silicon Carbide," *J. Am. Ceram. Soc.*, **65**(1), C27-C29 (1982).
30. B.-W. Lin, M.Imai, T.Yano, and T. Iseki,"Hot-Pressing of β-SiC Powder with Al-B-C Additives," *J. Am. Ceram. Soc.*, **69**(4), C67-C68 (1986).

Figure Captions

Figure 1. Alumina precursor coating development on the surface of SiC platelets. These SEM photos show the coating growth from negligible (1 hr., (a)) to complete surface coverage almost 1 μm thick (7 hrs., (c)).

Figure 2. SEM micrograph of the results of using high stoichiometric ratios of the reactants in solution to obtain fast-depositing amorphous coatings. The coatings are quickly precipitated first as a thin film (a), but are sensitive to cracking on drying (b).

Figure 3. Optical micrograph of the microstructure of the SiC/Al_2O_3-coated SiC platelet composite. Even in very highly loaded regions, the microstructure showed excellent density and platelet integrity.

Figure 4. SEM micrograph of an etched SiC-SiC platelet composite fabricated without coated platelets. The β grains have sintered and grown into the platelet, destroying any smooth interface between the two.

Figure 5. TEM micrograph of alumina coating along face of SiC platelet. The alumina coating is continuous and is typically 1-2 grains thick. The 4-H structure of the platelet (b) is kept intact during processing.

Figure 6. TEM micrograph of Al-B-C rich grain and larger SiC grains that we present within matrix. Electron diffraction, lattice imaging (b) and morphology indicate the presence of $Al_8B_4C_7$.

Figure 7. HREM micrograph of typical SiC-SiC grain boundary within the matrix. The grain boundaries are quite irregular; however, no amorphous interphase is observed.

Figure 8. SEM micrograph of a Vickers indent -induced crack path in the SiC composite. The platelets are prone to divert the crack, instead of fracturing.

Figure 9. SEM micrograph of a fracture surface on the SiC composite. The jagged surface as well as the evidence of platelet pullout testifies to higher measured toughnesses.

Figure 10. SEM micrograph of the rough, irregular platelets that resulted in poor fracture toughness values.

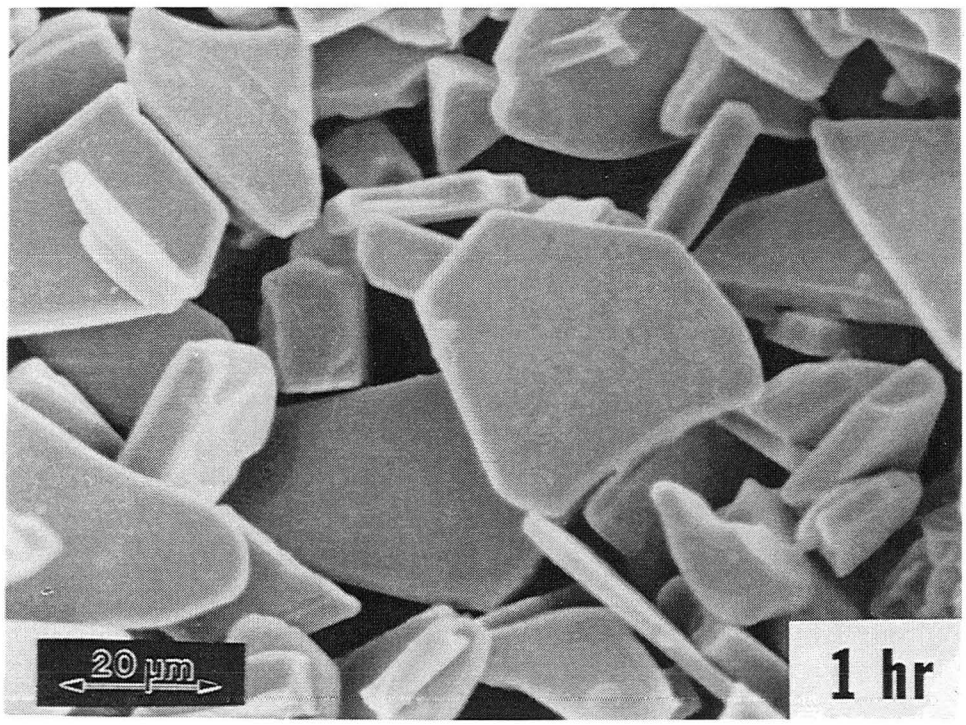

XBB 941-147

Figure 1a

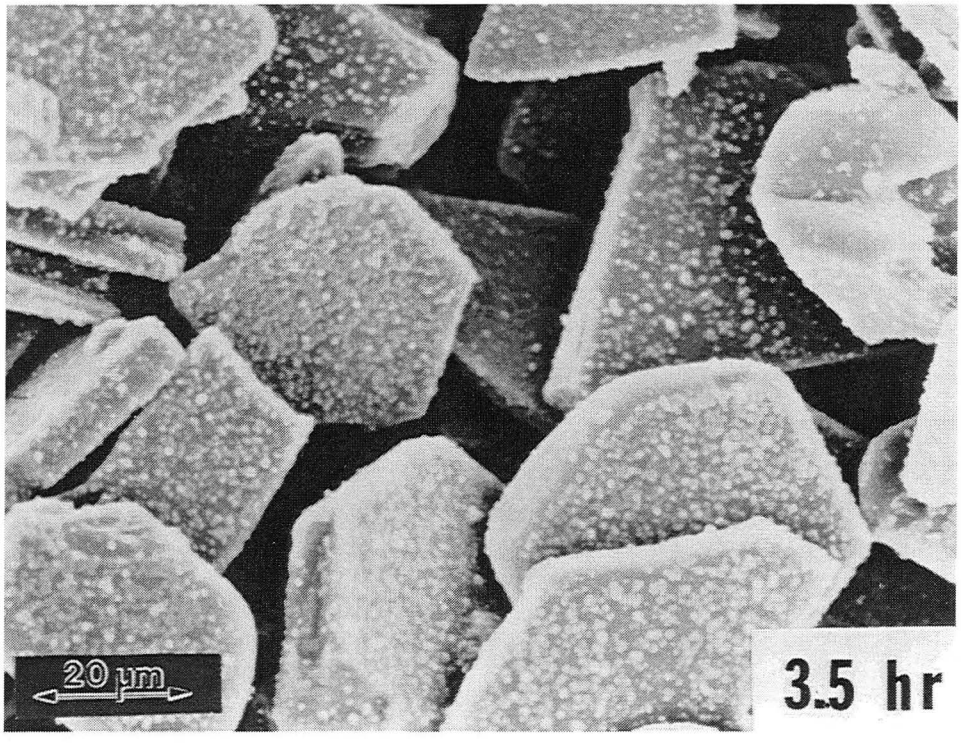

XBB 941-148

Figure 1b

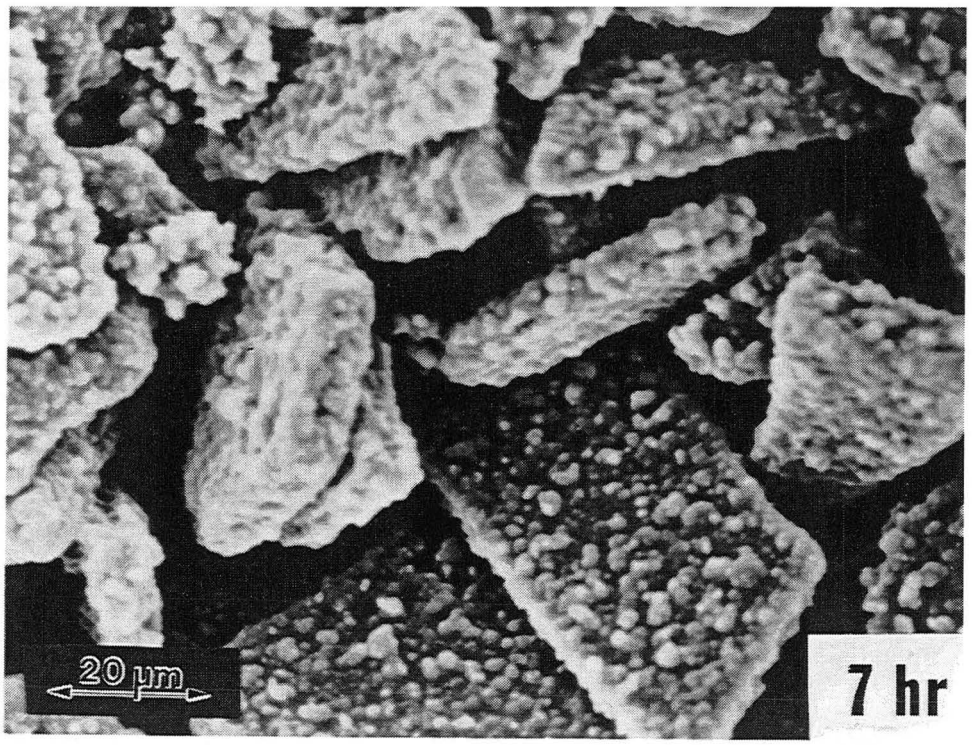

XBB 941-149

Figure 1c

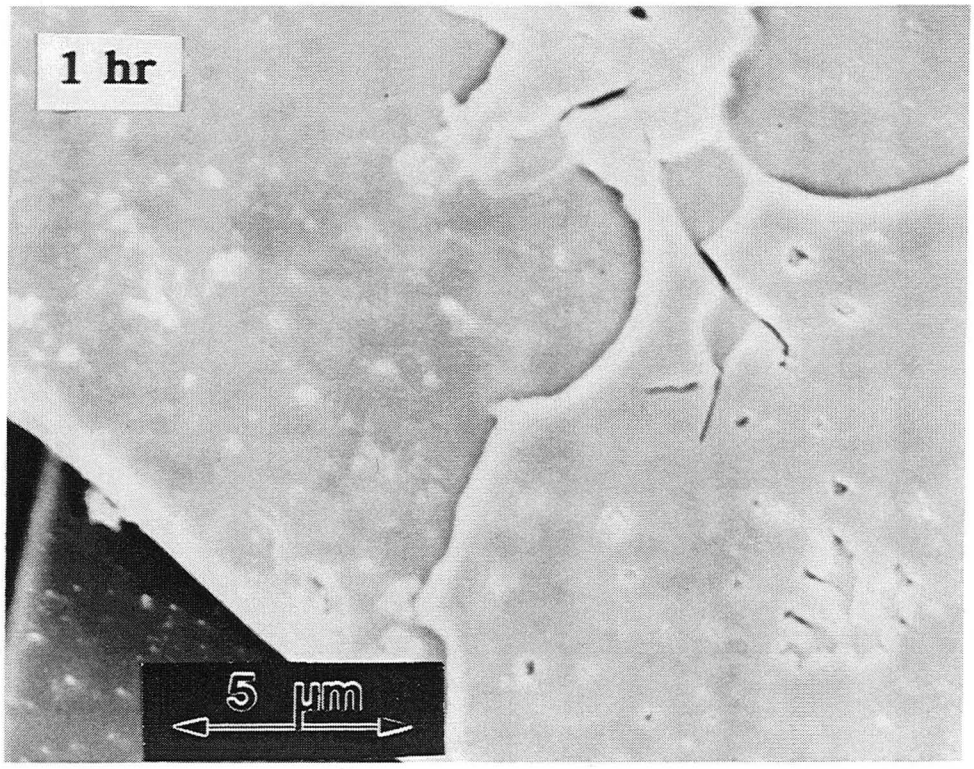

XBB 941-120

Figure 2a

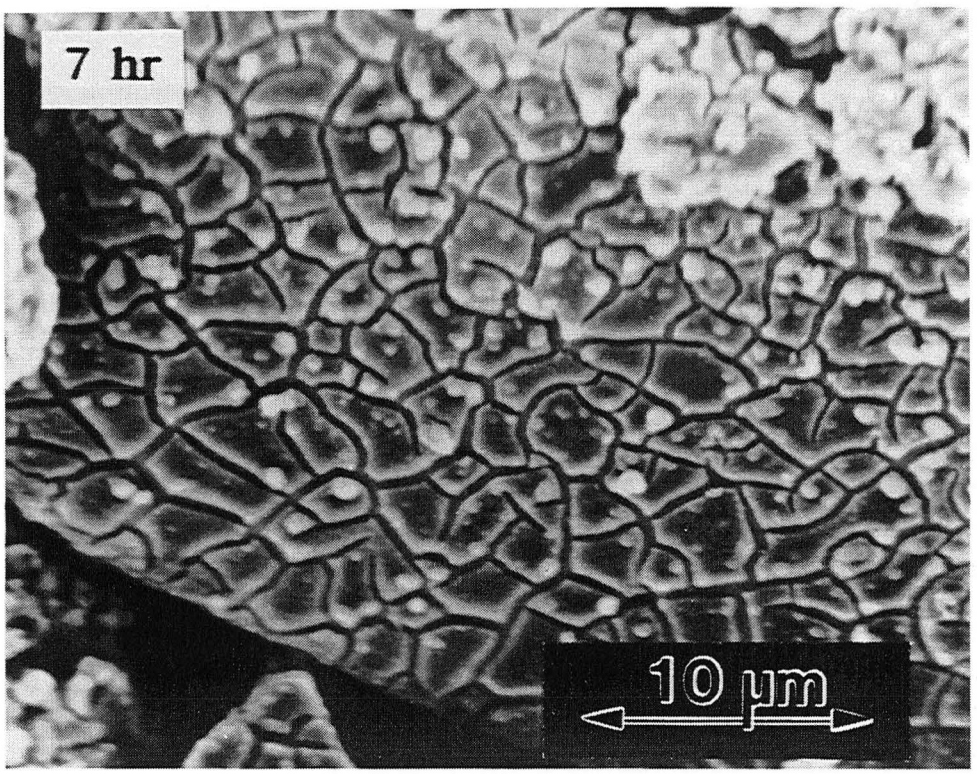

XBB 941-121

Figure 2b

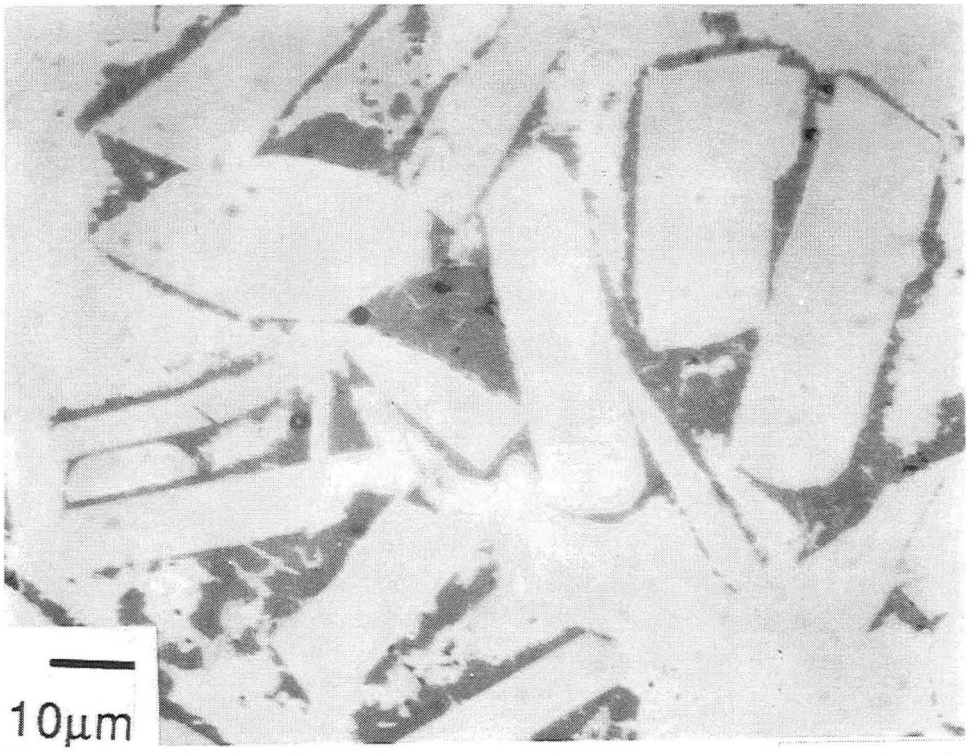

XBB 927-5280

Figure 3

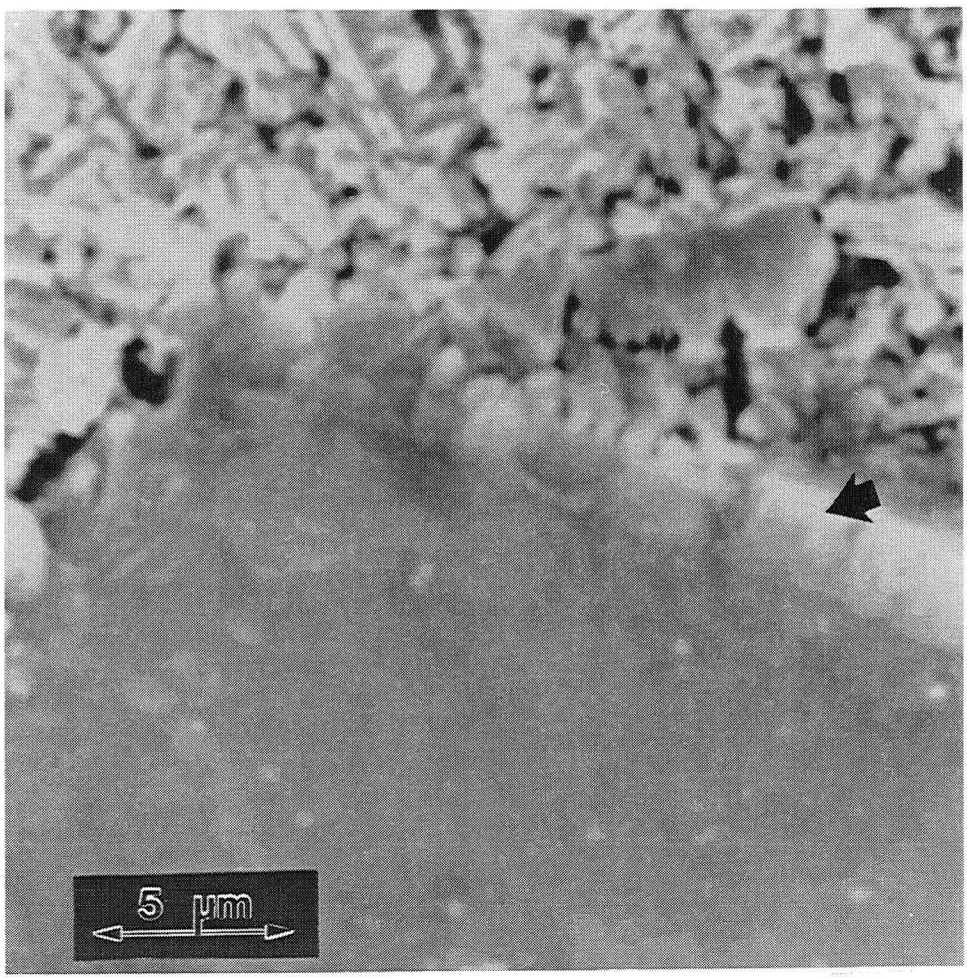

XBB 941-122

Figure 4

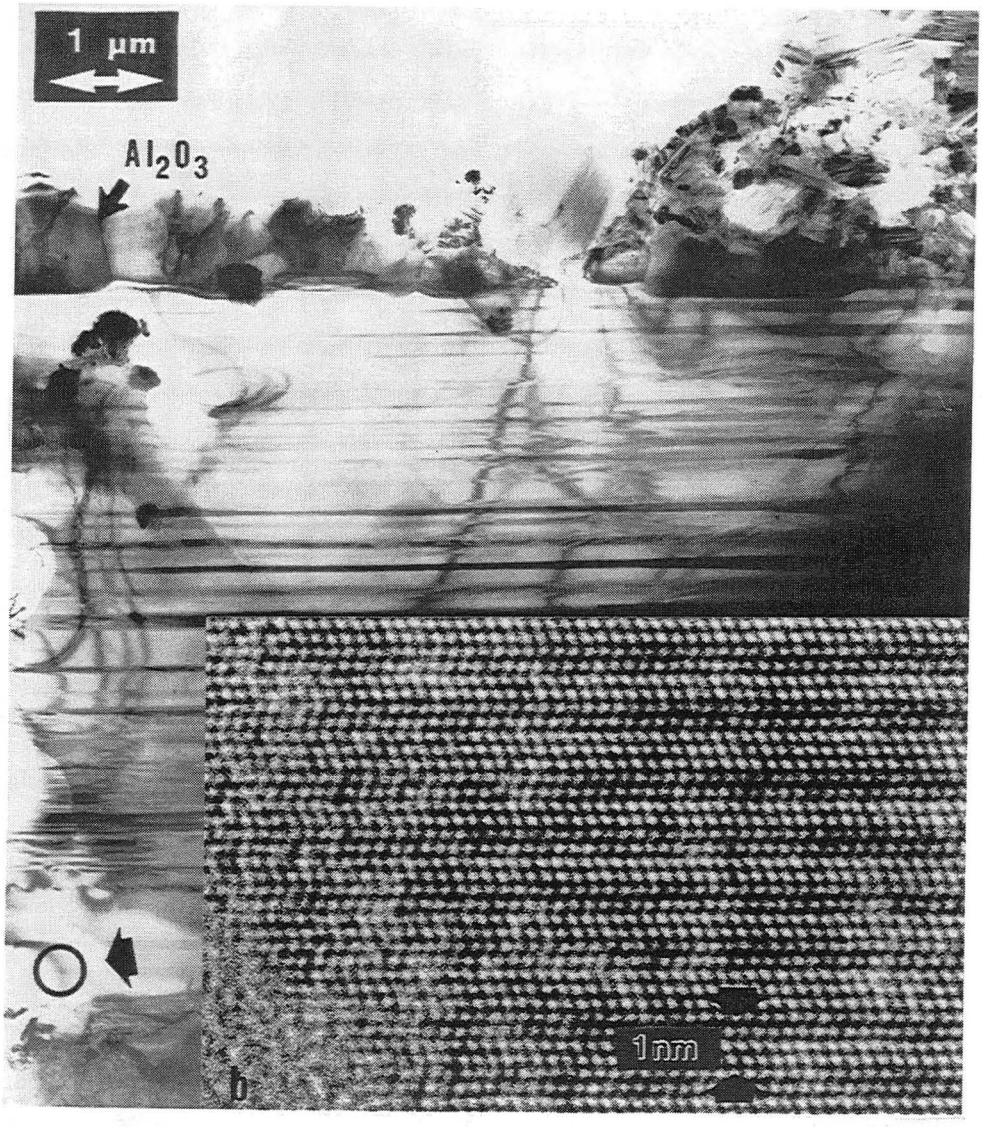

XBB 941-123

Figure 5

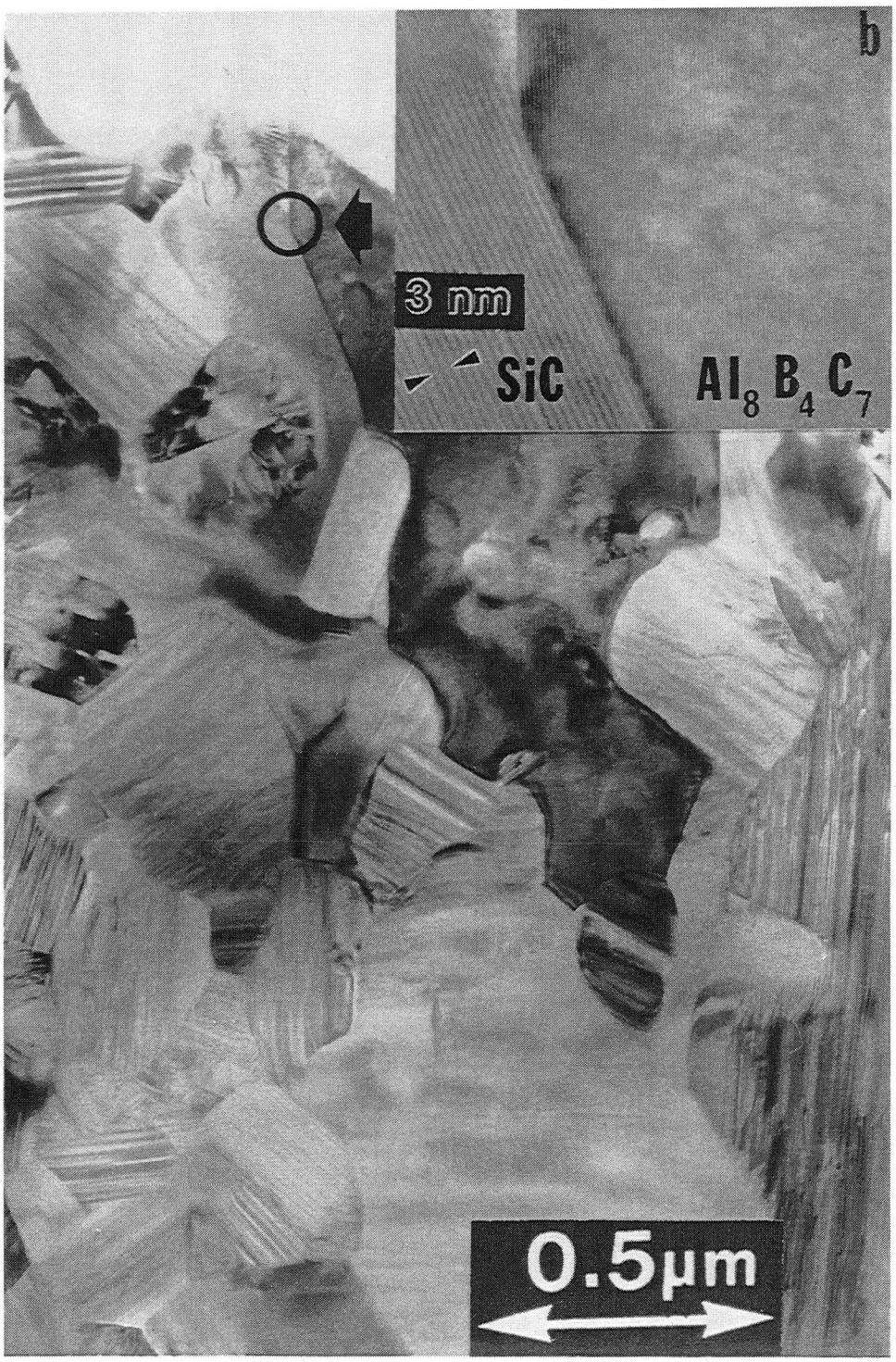

XBB 941-150

Figure 6

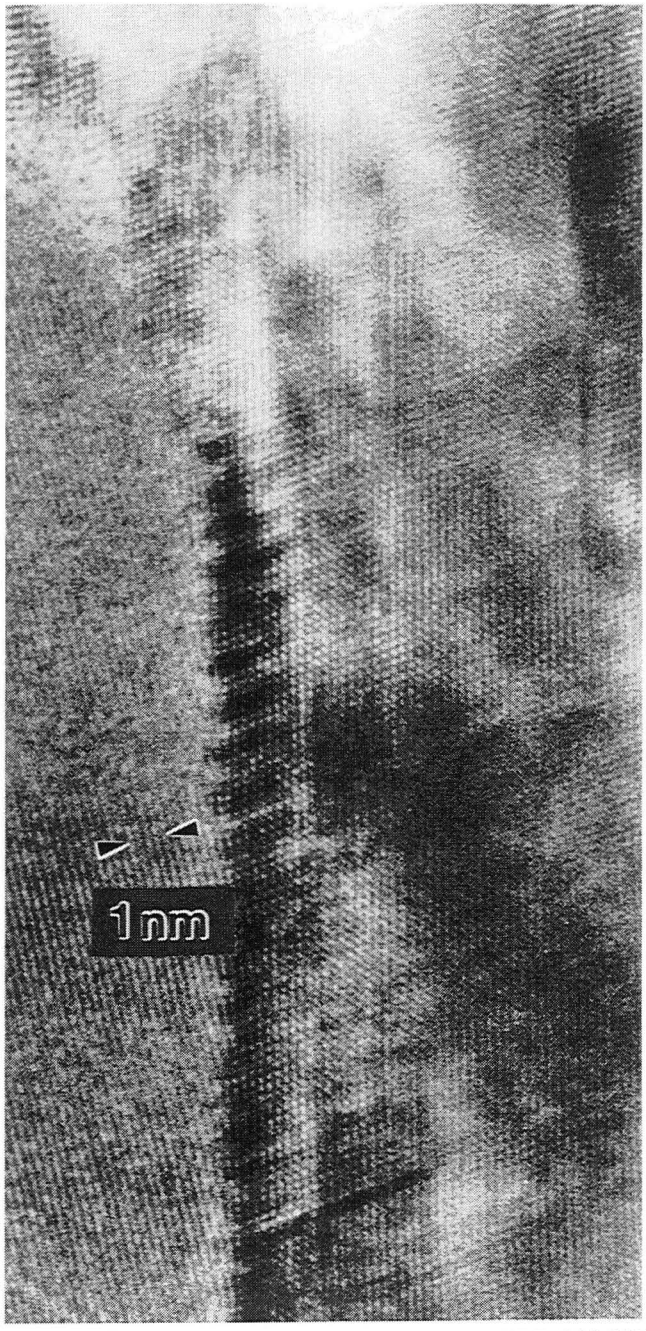

XBB 941-127

Figure 7

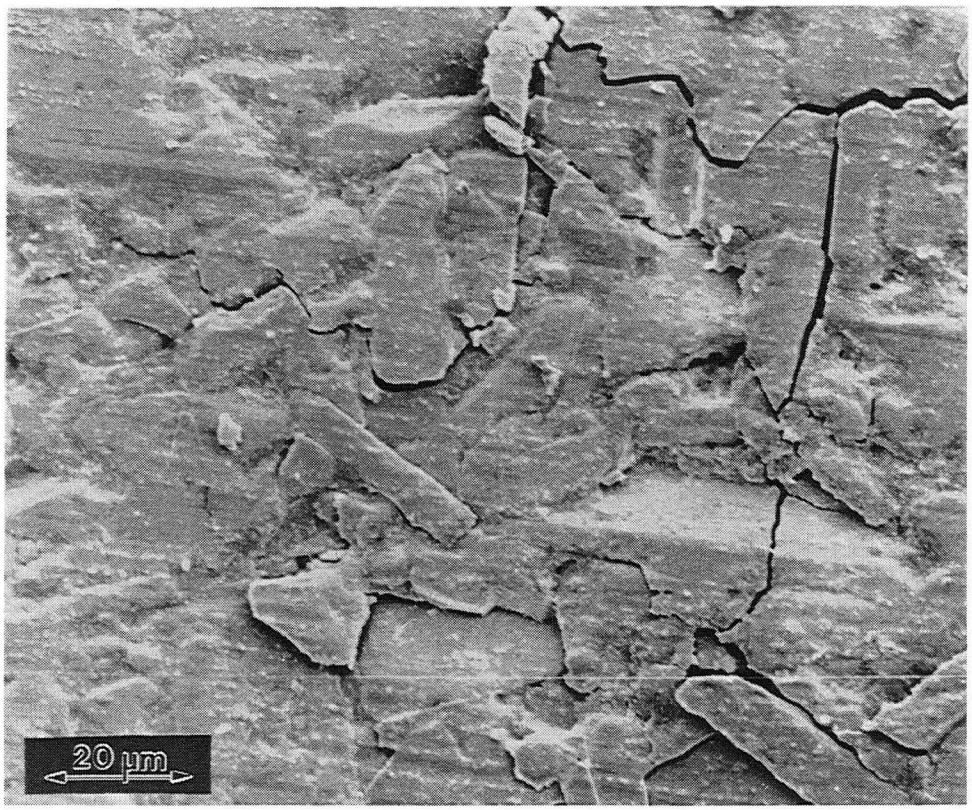

XBB 941-124

Figure 8

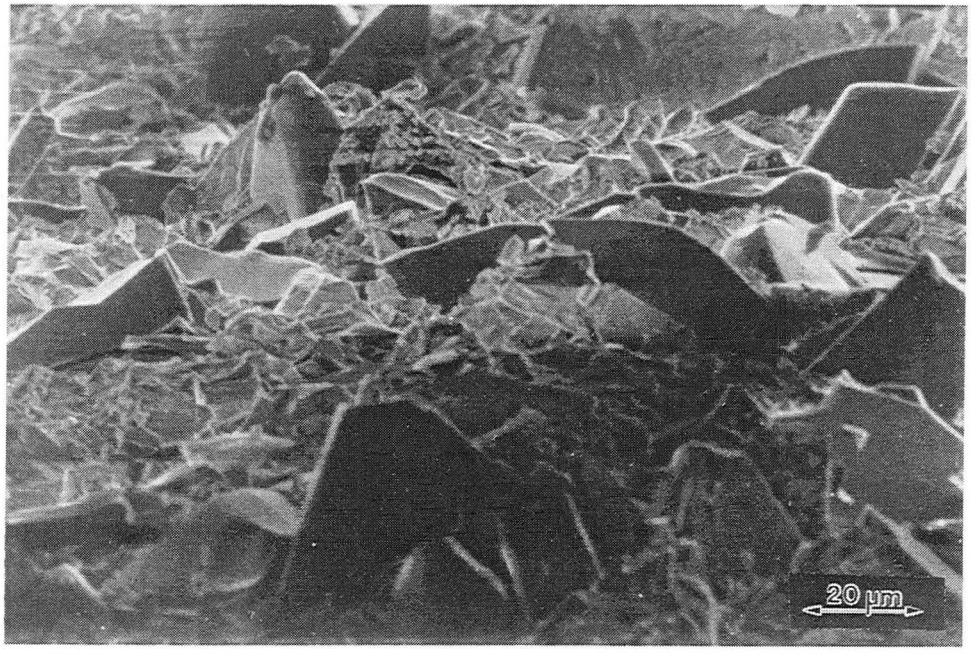

XBB 941-125

Figure 9

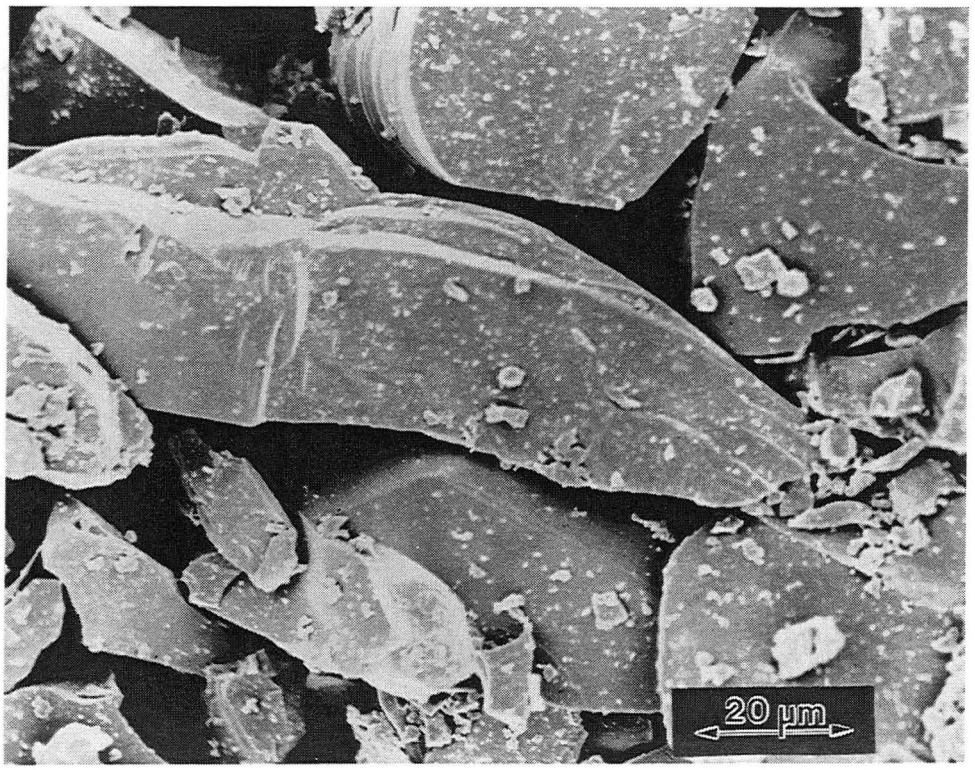

XBB 941-126

Figure 10

LAWRENCE BERKELEY LABORATORY
CENTER FOR ADVANCED MATERIALS
1 CYCLOTRON ROAD
BERKELEY, CALIFORNIA 94720